Semipolar InGaN/GaN Converters for Bright Green Emission and Stripe Light Emitting Diodes

Junjun Wang

Optically pumped green converter structures based on three-dimensional (3D) inverse pyramids were studied. The green emission intensity is determined by the conversion rate η_c and the absorption fraction η_a, indicating the InGaN/GaN quantum well (QW) crystal quality and its absorption capability, respectively. 15 was found to be the optimal QW number based the epitaxial condition for that series of green converters while a smaller number decreases η_a and a larger number degrades the QW quality and then decreases η_c. The thermal budget was found to be a critical issue for the InGaN/GaN QWs with a high indium content. A low InGaN growth temperature is required to achieve green emission leading to an inferior InGaN quality. A larger thickness, a higher TMIn molar flow and a higher reactor pressure are helpful to increase the InGaN well growth temperature for a certain emission wavelength. However, the higher reactor pressure results in worse InGaN quality finally. Conventional light emitting diodes (LEDs) based on 3D stripes were also investigated. The leakage current is related to the local high density defects generated within the active region penetrating the p-GaN, probably at the apex. It was successfully suppressed by reducing the QW number from 5 to 1 and inserting an AlGaN layer in the p-side of the structures in some distance to the QWs.

1. Introduction

The droop problem is typically identified as an electroluminescence (EL) efficiency maximum obtained at comparably small current densities of about $10\,\mathrm{A/cm^2}$ in GaN-based LEDs and a continuously decreasing efficiency at higher current densities. Various reasons like Auger recombination [1] and electron spill-over [2] are controversially discussed. One solution is to decrease the carrier concentration in the QWs, which requires either wider or more QWs. While semipolar structures allow wider QWs compared to polar structures, an increase of the number of QWs in LED structures is difficult due to the strongly different injection efficiencies of electrons and holes from the n- and the p-side of the diode, respectively. This issue is aggravated for high In content QWs but can be circumvented by optical excitation of carriers leading to the idea of luminescence conversion structures with green light emitting InGaN QWs optically pumped with a highly efficient blue LED [3]. Thus, a more homogeneous excitation of a larger amount of QWs can be achieved. Moreover, electron spill-over can be avoided in such electrically un-biased converter structures. In this work, we optimized conversion structures with semipolar InGaN/GaN QWs based on our 3D structure approach for bright green emission. The crystal quality of the InGaN/GaN QWs is the most critical issue for the conversion structure. Hence, they were

grown based on the 3D structure of GaN inverse pyramids beneficial from its well optimized growth condition.

It is also interesting to investigate the conventional electrically-excited LEDs on our 3D structures since it saves the complicated processing procedure to integrate the conversion structures with excitation blue LEDs. For the 3D LEDs, the 3D profile of each layer, especially the undoped GaN spacer and the p-(Al)GaN layer, needs to well controlled in order to achieve nice electrical properties which are limiting factors in the current status. Thus, the 3D structure of stripes was applied in the LEDs to make the 3D profile control easier as explained in [4].

2. Semipolar InGaN Converters for Bright Green Emission

2.1 Characterization

In order to measure the efficiency of the luminescence conversion, the green converters were characterized by transmission experiments. The light beam of a 405 nm blue laser diode is coupled into the converter samples in most cases from the sapphire-side of the wafer (forward excitation). The outcoupled blue and green light is detected from the epi-side. The absorption fraction η_a (the intensity ratio between the absorbed and incoupled blue light) and the conversion rate η_c (the intensity ratio between the converted green and the absorbed blue light) can be determined. They are figures of merit for the QW absorption capability and the QW emission quality, respectively. The relation between the converted green and incoupled blue light can be expressed by

$$I_\mathrm{converted,g} = I_\mathrm{incoupled,b} \times \eta_\mathrm{a} \times \eta_\mathrm{c} \ . \tag{1}$$

A similar sample without any InGaN/GaN QWs was taken as a reference to compensate the light back-scattering at each interface along the light path since the light incoupling and outcoupling efficiencies are equal for the green converter and the reference sample. The absorption fraction η_a is calculated as

$$\eta_\mathrm{a} = \frac{I_\mathrm{outcoupled,b,r} - I_\mathrm{outcoupled,b}}{I_\mathrm{outcoupled,b,r}} \tag{2}$$

by evaluating the intensities of the outcoupled blue light for the green converter and the reference sample, indicated by $I_\mathrm{outcoupled,b}$ and $I_\mathrm{outcoupled,b,r}$, respectively. Assuming that the outcoupling efficiency η_e is equal for the blue and green light, the calculation of the conversion rate η_c can be expressed as

$$\eta_\mathrm{c} = \frac{I_\mathrm{converted,g} \times \eta_\mathrm{o}}{I_\mathrm{absorbed,b} \times \eta_\mathrm{o}} = \frac{I_\mathrm{outcoupled,g}}{I_\mathrm{outcoupled,b,r} - I_\mathrm{outcoupled,b}} \ . \tag{3}$$

The overall intensity of the outcoupled light in front of the sample is achieved by integrating the light intensity over the semispheric surface. As shown in Fig. 1, the outcoupled blue light is distributed center-symmetrically with a six-fold pattern as a consequence of our hexagonal pyramidal surface structure. Hence, the mapping of the area normalized

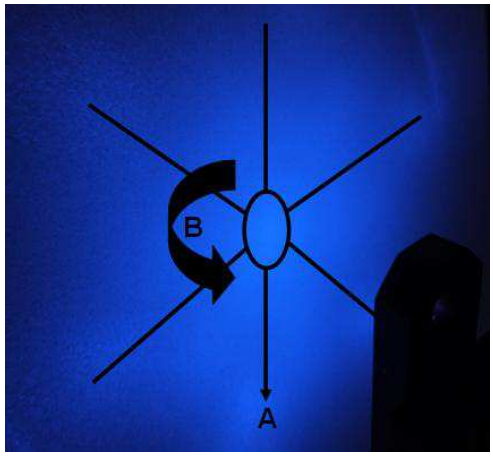

Fig. 1: The outcoupled blue light intensity distribution of the reference sample on a screen. The six straight lines show the six-fold pattern with the center indicated by the ellipse. Two dimensional angle-resolved measurements are performed along the radial (A) and circular (B) directions.

light intensity is performed via angle-resolved measurements in the radial direction indicated as A and the circular direction indicated by the rotation angle B in Fig. 1. The case of the outcoupled green light is even simpler since its distribution is center-symmetrical and constant along the circular direction.

The absorption coefficient α can be calculated from the absorption fraction η_a by

$$1 - \eta_\mathrm{a} = e^{-2\alpha n d} \tag{4}$$

where n and d represent the number and the thickness of the QWs, respectively. Since our semipolar QWs are tilted by 60 ° with respect to the substrate surface, the path of the blue light through the QWs is actually twice of the QW thickness which gives the factor of 2 in 4. With the same QW number, the doubled light path in our tilted QWs compared to the planar ones results in a strong absorption of the blue light in our structures.

2.2 Results and discussion

As mentioned above, the possibility to increase the number of QWs is a significant advantage of such optically pumped structures, which increases the overall absorption of the excitation light and hence potentially the green light intensity. However, two things must be considered when doing so: On one hand, late grown QWs may have lower quality as they are grown on already strained sub-layers. On the other hand, early grown QWs are longer subjected to high temperatures which may degrade their quality. Hence, an optimum has to be found concerning the number of QWs. To this end, we have grown three samples (samples 1, 2 and 3) with 10, 15 and 20 QWs, respectively, all emitting at the same wavelength of 505 nm. Indeed, the absorption fraction η_a rises with increasing QW number as expected, exceeding 90 % for the samples with 15 and 20 QWs. Although the electron and hole distributions are much more homogeneous for optically pumped green

converters compared to electrical pumping in conventional LEDs, the amount of electrons and holes within the QWs decreases exponentially with respect to the penetration depth of the blue pump light. Thus, the overall performance will depend more strongly on the quality of the QWs closer to the excitation source. Samples 1 and 2, with 10 and 15 QWs, respectively, have similar values for η_c, 4.9 % and 5.1 %, indicating comparable QW quality and the higher number of QWs results in a brighter total green emission. However, for sample 3 the further addition of 5 QWs leads to a reduction of η_c by 0.9 % compared to sample 2 indicating an inferior crystalline quality for the higher number of QWs which counters and outweighs the higher absorption of blue light. As explained above, this may be caused by not only the larger thermal load experienced by early grown QWs during the longer overgrowth but also the more defective late grown QWs. With the epitaxy conditions for this series of samples, sample 2 has the strongest green emission achieving a balance between the parameters η_a and η_c.

Table 1: Result of the transmission experiment for samples 1–5 with forward excitation ($\lambda = 505\,\mathrm{nm}$).

Sample no.	1	2	3	4	5
QW number	10	15	20	2×5	4×5
η_a	85 %	92 %	95 %	87 %	93 %
α ($10^5\,\mathrm{cm}^{-1}$)	3.8	3.4	2.9	4.0	2.6
η_c	4.9 %	5.1 %	4.2 %	2.6 %	2.6 %

In order to reduce strain related defects and to improve the quality of the late grown QWs, groups of 5 QWs each were separated by inserting about 50 nm GaN, thus reducing the average In content of the active layer. Two samples with 2×5 QWs and 4×5 QWs (samples 4 and 5 in Table 1) were produced. While the samples with the same number of QWs (samples 1 and 4; samples 3 and 5) have similar values of η_a, the samples with separated groups of QWs have substantially decreased values for η_c. This is attributed to the extra thermal load caused by the growth of the GaN layer between each two groups of 5 QWs which seems to be more important than the reduced strain.

All of the 5 samples (samples 1–5) have similar values for the absorption coefficient α which confirms comparable absorption capability for the InGaN material with the same indium content.

As discussed above, the absorption in the QWs farther from the excitation source is much weaker than that in the ones close to it. Hence, the QWs with better quality should be placed closer to the excitation source to enhance the green emission intensity. When the green converter is placed with its epi-side facing the 405 nm laser, most of the pump light is absorbed in the topmost QWs and the measured light leaves the sample from the sapphire-side. We refer to such an experimental setup as backward excitation while the previously mentioned transmission experiment is named forward excitation. As seen in Table 2, η_a is pretty similar for the forward and backward excitation, respectively, for all

5 samples. Interestingly, η_c is enhanced by nearly 90 % in backward excitation for sample 3. This result shows that the late grown QWs which are not subjected to a large thermal load have a better quality than the early grown ones and further optimization for samples with high numbers of QWs should specifically address the issue of thermal budget.

Table 2: Result of the transmission experiment for samples 1–5 with backward excitation ($\lambda = 505\,\mathrm{nm}$).

Sample no.	1	2	3	4	5
QW number	10	15	20	2×5	4×5
η_a	89 %	91 %	94 %	89 %	95 %
α ($10^5\,\mathrm{cm}^{-1}$)	4.4	3.2	2.7	4.4	3.1
η_c	8.6 %	8.2 %	7.9 %	3.7 %	3.2 %

For a long emission wavelength above 500 nm, a low growth temperature below 800 °C is required for the InGaN wells leading to a degraded material quality. We tried to improve the InGaN material quality by increasing its growth temperature while a larger InGaN well thickness, a higher TMIn (trimethylindium) flow rate and a higher reactor pressure are applied to compensate the emission wavelength blueshift. For this purpose, green converters with 5 InGaN/GaN QWs were fabricated under different InGaN growth conditions.

Table 3: Result of the transmission experiment for samples 6–8 with forward excitation ($\lambda = 510\,\mathrm{nm}$).

Sample no.	6	7	8
nominal QW thickness (nm)	2.5	3.5	5.0
InGaN growth T (°C)	710	714	721
η_a	51 %	65 %	72 %
α ($10^5\,\mathrm{cm}^{-1}$)	2.9	3.0	2.5
η_c	6.9 %	6.9 %	7.7 %

As listed in Table 3, three samples (samples 6, 7 and 8) were prepared with a nominal InGaN well thickness of 2.5 nm, 3.5 nm and 5.0 nm, respectively. η_a rises with increasing nominal InGaN well thickness, in other words, with increasing effective total InGaN thickness while the intrinsic property of the InGaN material α is quite similar among these three samples. The required InGaN growth temperature is higher for thicker QWs to obtain a certain emission wavelength. In the case of c-plane InGaN/GaN QWs, the luminescence efficiency drops with increasing QW thickness caused by the quantum-confined Stark effect outweighing the benefit from the higher InGaN growth temperature. Owing to the reduced piezoelectric field, this negative effect is not as strong in our semipolar

InGaN/GaN QWs as that on the c-plane ones. η_c is 6.9 % for both of samples 6 and 7 and increases to 7.7 % for sample 8. So a larger QW thickness is helpful to enhance η_a and η_c at the same time.

Table 4: Result of the transmission experiment for samples 9–11 with backward excitation ($\lambda = 518\,\mathrm{nm}$).

Sample no.	9	10	11
TMIn molar flow rate (µmole/min)	26.4	39.8	53.0
InGaN growth T (°C)	755	782	790
η_a	90 %	87 %	88 %
α ($10^5\,\mathrm{cm}^{-1}$)	4.6	4.0	4.2
η_c	5.5 %	10.3 %	7.8 %

As listed in Table 4, three samples (samples 9, 10 and 11) were prepared with a TMIn molar flow rate of 26 µmole/min, 40 µmole/min and 53 µmole/min, respectively. The required InGaN growth temperature to achieve the emission wavelength of 518 nm is enhanced by about 17 °C when the TMIn molar flow rate increases from 26 µmole/min to 40 µmole/min leading to almost a doubled value of η_c. However, further enhancement of TMIn molar flow reduces η_c probably due to changes in microscopic InGaN growth mechanism.

Table 5: Result of the transmission experiment for samples 12 and 13 with backward excitation ($\lambda = 510\,\mathrm{nm}$).

Sample no.	12	13
reactor pressure (hPa)	200	400
InGaN growth T (°C)	758	765
η_a	83 %	85 %
α ($10^5\,\mathrm{cm}^{-1}$)	3.5	3.8
η_c	12.0 %	6.9 %

As listed in Table 5, two samples (samples 12 and 13) were prepared with reactor pressures of 200 hPa and 400 hPa, respectively. A high reactor pressure can indeed increase the required InGaN growth temperature for the emission wavelength of 510 nm, but results in a smaller η_c indicating an inferior InGaN crystal quality.

3. Stripe Light Emitting Diodes

In this section, we investigate conventional electrically pumped LEDs with semipolar InGaN/GaN QWs on the side facets of periodic stripes.

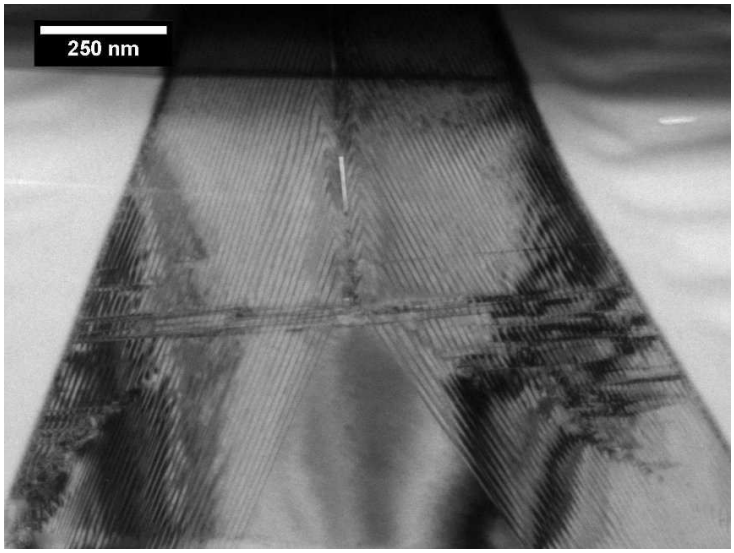

Fig. 2: Cross-sectional TEM image of a converter structure with 40 InGaN/GaN QWs.

The stripe LED with 5 InGaN/GaN QWs generates an output power of 340 µW at 58 mA and breaks down afterwards with increasing current. The leakage current at a reverse bias of 5 V is as high as ∼3 mA. A high density of defects through the diode may be responsible for the big leakage current. A cross-sectional TEM (transmission electron microscope) image of a converter structure with 40 InGaN/GaN QWs shows a high defect density within the active region at the stripe apex and stacking fault arrays originated at the stripe apex running horizontally (Fig. 2). It was reported that AlN layers can terminate such stacking faults [5]. Hence, we aimed to block the leakage current by including an AlGaN layer within our stripe LED structure either directly above the undoped GaN spacer or above ∼50 nm Mg:GaN (Fig. 3). In the former case, the AlGaN layer performs simultaneously as electron blocking layer (EBL). In the latter case, the tip is better

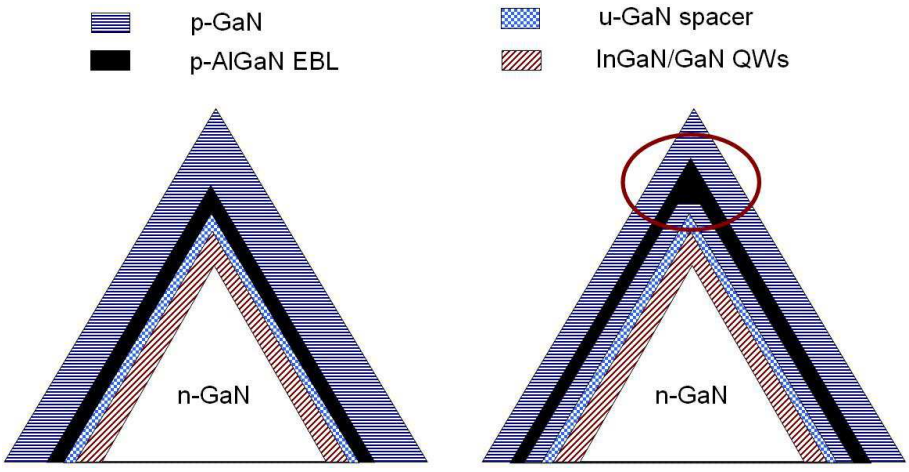

Fig. 3: Schematic structures for the stripe LEDs with an AlGaN layer directly on undoped GaN spacer (left) and above ∼50 nm Mg:GaN (right).

blocked by a thicker AlGaN layer there: Mg doing induces lateral growth [6] resulting in a plateau on the c-plane surface after ∼50 nm Mg:GaN growth. The following AlGaN layer grows more vertically, rebuilding the sharp tip and leading to a larger thickness there. The leakage current stays in the same order or even gets higher with the addition of the AlGaN EBL while it is successfully reduced from ∼3 mA to ∼0.3 mA by inserting the up-shifted AlGaN layer (Table 6). With the heavily reduced leakage current, the LED with the up-shifted AlGaN layer shows quite promising performance in EL. It works stably up to ∼120 mA without the diode breakdown indicating suppressed local current crowding, especially at the tip (Fig. 4). However, the LED with the up-shifted AlGaN layer still has a lower output power than the one without any AlGAN layer, probably due to a reduced hole injection. So further optimization is required for the Al-content, thickness and position of the up-shifted AlGaN layer.

Table 6: Leakage currents at −5 V for LEDs with 5 QWs (without any AlGaN layer, with the AlGaN EBL and the up-shifted AlGaN layer) and with a single QW.

	no AlGaN	AlGaN EBL	up-shifted AlGaN	no AlGaN
QW number	5	5	5	1
Leakage current at −5 V	3 mA	5 mA	0.3 mA	1 mA

A single-QW LED should have a smaller defect density within the active region compared to a 5QW one due to the reduced strain. This may lead to a lower leakage current. One single-QW LED was produced without any AlGaN layer which may affect the hole injection negatively. Indeed, this sample has a smaller leakage current of ∼1 mA compared to the 5QW LED as expected (Table 6). This LED also gives a quite high output power of 0.53 mW at 70 mA in EL (Fig. 4).

As discussed, conventional Mg doping induces lateral growth resulting in a plateau on the Mg:GaN surface with the sharp Si:GaN apex underneath. When the contact metal gets direct contact to the QWs, short circuits can occur. To overcome this problem, the technique of 'pulse doping' (the metalorganics and NH_3 are supplied alternatively in pulses) was applied for all the stripe LEDs mentioned above to push the Mg:GaN growth vertically [6]. The Mg:GaN was grown with conventional doping for the bottom and top layers, but with pulse doping in the middle layer. The up-shifted AlGaN layer was placed on top of conventionally-doped Mg:GaN. However, the Mg:GaN growth rate with the pulse doping technique is only about 1/3 of that of the conventional Mg:GaN. The thermal load is very critical for the green InGaN/GaN QWs degrading the InGaN crystal quality heavily via indium segregation [7]. The required longer growth time of the pulse-doped p-GaN aggravates the thermal load for the underlying InGaN/GaN QWs. Therefore, we have developed a procedure called 'triple p-GaN' which can push the vertical Mg:GaN growth without decreasing the growth rate. It starts with a high Mg doping level in order to achieve sufficient p-conductivity during which a c-plane plateau is developed. Then, a thin Mg:GaN layer with a low Mg doping level rebuilds the sharp apex, preventing any direct contact between the QWs and the metal contact. The third Mg:GaN layer is

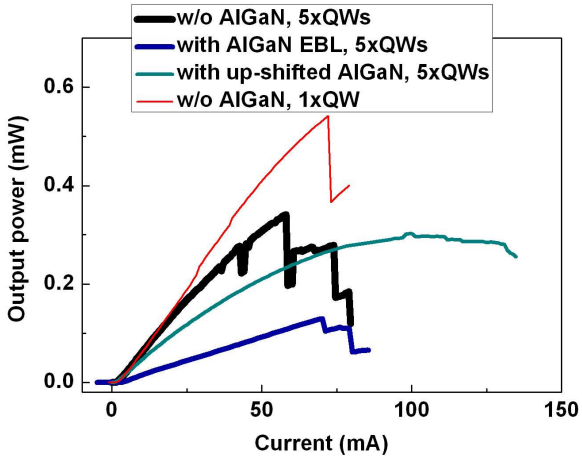

Fig. 4: EL output power against current for all the samples in Table 6.

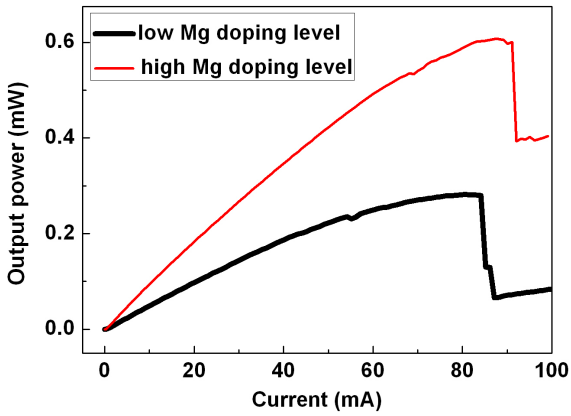

Fig. 5: EL output power against current for 5QW stripe LEDs with the up-shifted AlGaN layer and the triple p-GaN layer, one with a higher Mg doping level in the middle p-GaN layer compared to the other.

highly doped to obtain good contact properties. Two 5QW stripe LEDs were prepared with the up-shifted AlGaN layer and the triple p-GaN. The Mg doping level is increased for the second LED in the middle slightly-doped p-GaN layer. Strongly reduced leakage currents of ∼30 µA and ∼15 µA, respectively, have been obtained. In order to completely understand these promising results, more investigations, for example TEM and µ-EL, are currently underway. As seen in Fig. 5, the enhanced Mg doping level in the middle slightly-doped p-GaN layer doubled the output power in EL due to improved hole injection. The LED with higher Mg doping level in the middle p-GaN layer gives an output power of 0.54 mW at 70 mA and works stably up to 90 mA.

4. Conclusion

In order to optimize luminescence conversion structures with semipolar QWs for the generation of green light, we varied several parameters of our QW structures. We found an optimal QW number of 15 based on the epitaxy conditions for that series of samples with different QW numbers. Obviously, a much smaller number of semipolar InGaN/GaN QWs is necessary to achieve sufficient blue light absorption compared to c-plane ones [3]. The thermal budget is a very critical issue for the InGaN crystal quality. A high InGaN growth temperature is beneficial for the InGaN crystal quality. In order to enable a higher growth temperature of the QWs, we studied structures with thicker QWs, a higher TMIn molar flow rate and a higher reactor pressure aiming at the same emission wavelength. Both, absorption fraction η_a and conversion rate η_c increase with thicker QWs. With an increased TMIn molar flow rate, $\eta_c = 10.3\,\%$ was realized at the emission wavelength of 518 nm with $\eta_a = 87\,\%$. A higher reactor pressure can help increase In uptake and hence to increase the InGaN growth temperature but eventually results in an inferior InGaN crystal quality.

In electrically driven semipolar LED structures, we observed that the leakage current is smaller in single-QW stripe LEDs than in 5QW ones due to the reduced defect density, especially at the stripe apex. We successfully decreased the leakage current by incorporating an AlGaN layer in the p-side of the structures in some distance to the QWs. In order to improve the shape of the GaN:Mg layer near the apex of our stripes, we applied special techniques like pulse doped p-GaN and triple p-GaN to push the Mg:GaN growth vertically. The growth rate of the triple p-GaN is 3 times of that of the pulse doped p-GaN thus reducing the thermal budget for the underlying InGaN/GaN QWs. A higher Mg doping level in the middle p-GaN layer of the triple p-GaN doubled the output power in EL due to improved hole injection.

Acknowledgment

I gratefully acknowledge the scientific and technical support from I. Schwaiger, W. Mierlo, D. Zhang, M. Hocker, T. Meisch, R. Leute and I. Tischer. This work was financially supported by the German Federal Ministry of Education and Research (BMBF).

References

[1] Y.C. Shen, G.O. Mueller, S. Watanabe, N.F. Gardner, A. Munkholm, and M.R. Krames, "Auger recombination in InGaN measured by photoluminescence", *Appl. Phys. Lett.*, vol. 91, pp. 141101-1–3, 2007.

[2] M.H. Kim, M.F. Schubert, Q. Dai, J.K. Kim, E.F. Schubert, J. Piprek, and Y. Park, "Origin of efficiency droop in GaN-based light-emitting diodes", *Appl. Phys. Lett.*, vol. 91, pp. 183507-1–3, 2007.

[3] B. Galler, M. Sabathil, A. Laubsch, T. Meyer, L. Hoeppel, G. Kraeuter, H. Lugauer, M. Strassburg, M. Peter, A. Biebersdorf, U. Steegmueller, and B. Hahn, "Green high-power light sources using InGaN multi-quantum-well structures for full conversion", *Phys. Status Solidi C*, vol. 8, pp. 2369–2371, 2011.

[4] J. Wang, "3D GaInN/GaN-based Green Light Emitters", *Annual Report 2011*, pp. 33–40. Ulm University, Institute of Optoelectronics.

[5] A. Dadgar, R. Ravash, P. Veit, G. Schmidt, M. Müller, A. Dempewolf, F. Bertram, M. Wieneke, J. Christen, and A. Krost, "Eliminating stacking faults in semi-polar GaN by AlN interlayers", *Appl. Phys. Lett.*, vol. 99, pp. 021905-1–3, 2011.

[6] T. Wunderer, P. Brückner, B. Neubert, F. Scholz, M. Feneberg, F. Lipski, M. Schirra, and K. Thonke, "Bright semipolar GaInN/GaN blue light emitting diode on side facets of selectively grown GaN stripes", *Appl. Phys. Lett.*, vol. 89, pp. 041121-1–3, 2006.

[7] Y.T. Moon, D.J. Kim, K.M. Song, C.J. Choi, S.H. Han, T.Y. Seong, and S.J. Park, "Effects of thermal and hydrogen treatment on indium segregation in InGaN/GaN multiple quantum wells", *J. Appl. Phys.*, vol. 89, pp. 6514–6518, 2001.